Cold Regions Science and Technology 97 (2014) 159–169

Contents lists available at ScienceDirect

Cold Regions Science and Technology

journal homepage: www.elsevier.com/locate/coldregions

Retarding avalanches in motion with net structures

Engelbert Gleirscher *, Jan-Thomas Fischer

Federal Research and Training Centre for Forests, Natural Hazards and Landscape — BFW, Department of Natural Hazards, Innsbruck, Austria

ARTICLE INFO

Article history:
Received 16 November 2012
Received in revised form 30 July 2013
Accepted 12 August 2013

Keywords:
Snow net
Avalanche
Protection measure
Granular experiment
Mesh size
Runout length

ABSTRACT

Steel wire rope nets have become a common protection measure against snow avalanches in Europe, as they can prevent a release in potential starting zones. A novel approach in this context, is to retard the movement of an avalanche after it has been initiated. A full scale structure, the so-called Snowcatcher, was installed and instrumented with several load measuring pins, which record the dynamic loads caused by an avalanche. The motivation of the measurements is to observe the influence of net structures on snow avalanches. In the lab, scaled granular experiments were performed in two set-ups, investigating the influence of i) the net barrier angle and ii) the mesh size of the net. For both set ups various experiments with different chute inclinations were performed. The results from measuring the front velocities and flow depths showed that higher chute angles are accompanied with both, higher flow velocities and Froude numbers. Experiments with different net barrier angles showed that the effectivity increases with higher chute inclinations. Furthermore the results indicate that different barrier angles slightly influence the effectivity, e.g. for small chute inclinations, nets perpendicular to the flow direction lead to lower effectivities than inclined nets. Experiments with different mesh sizes indicate a velocity dependency of the effectivity corresponding to a certain ratio of mesh to grain size. Smaller mesh sizes in the range of the maximal particle grain size lead to an obstruction of the net, acting as a solid barrier and therefore reaching best effectivity, notwithstanding overflows. For large mesh sizes the effectivity of the net barrier increases with a higher velocity of the flow.

1. Introduction

Permanent avalanche mitigation measures are either constructed in the release zone (e.g. snow bridges) or in the lower avalanche path/runout zone (e.g. dams) (Margreth et al., 2011; Pudasaini and Hutter, 2007). Under certain topographical conditions one advantage of constructing measures in the runout zone, as opposed to the release zone, is the possible reduction of construction lengths, due to an often smaller avalanche width. This has a major impact on the project implementation, especially with regard to space and time savings, resulting in lower construction costs and often less ecological impact. At present, the most common method of retarding an avalanche in motion are avalanche protection dams, which were subject to several scientific studies (e.g. Baillifard, 2007; Domaas et al., 2002; Hákonardóttir, 2004; Johannesson et al., 2009). Herein a new system is proposed, using flexible wire rope nets: the Snowcatcher presents a viable alternative to avalanche dams for areas endangered by smaller avalanches. Flexible rope nets for the protection against rockfall are common and have previously been investigated, (Gottardi and Govoni, 2010; Peila and Ronco, 2009; Volkwein, 2005). While rockfall nets are optimized to absorb high punctual impact energies, avalanche pressure acts over a much larger area and longer time period (Margreth and Roth, 2008). Therefore results from rockfall and avalanche experiments on flexible wire rope nets can hardly be compared to one another. In Wendeler et al. (2006) a test site instrumented with flexible rope nets for debris flow mitigation is presented. A static system without posts is constructed in a narrow gully. Forces on the flexible net are recorded during debris flow events and are compared with numerical simulations. Events showed that the barrier could stop parts of the debris flow. Since debris flows are generally comparable with snow avalanches, such a system could be applied to snow avalanche mitigation (Nicot et al., 2004; Roth et al., 2010). A debris flow mitigation barrier that is constructed with supporting frames, similar to the prototype presented here, is described in Bichler et al. (2012): The barrier is instrumented with load gauges, but no data could be analyzed since no event has occurred to date. In summary it can be stated, that several tests on flexible wire rope nets have been performed and seem to confirm the desired retarding influence on rockfall and debris flow. However, our goal is to analyze the retarding influence of net barriers on granular flows, such as snow avalanches, by comparing a characteristic retardation length in granular experiments. This retardation length is related to the runout length. To our knowledge this topic has not been accounted for in previous works. In the case of snow avalanches only little information is available on the retardation behavior of steel wire rope nets. Therefore a full scale prototype of the Snowcatcher was instrumented with several load measuring pins, which record the dynamic loads

* Corresponding author at: Federal Research and Training Centre for Forests, Natural Hazards and Landscape — BFW, Department of Natural Hazards, Rennweg 1, A-6020 Innsbruck, Austria. Tel.: +43 512 573933 5103.
E-mail address: Engelbert.Gleirscher@uibk.ac.at (E. Gleirscher).

0165-232X/$ – see front matter © 2013 Elsevier B.V. All rights reserved.
http://dx.doi.org/10.1016/j.coldregions.2013.08.007

caused by an avalanche. The main purpose of this setup is to measure normal and shear forces in the net supporting frame and the cable forces. The field tests were limited to force measurements and therefore restricted statements regarding the effectivity of a net barrier with respect to changing net set-ups are available.

Lab experiments were performed to analyze the influence of the net barrier on granular flows. Approved methods, such as velocity measurements and flow depth measurements, were used to carry out scaled granular experiments in order to simulate avalanches in the lab. To date, experiments have mainly been performed to investigate the interaction of granular flows with solid structures. Tai et al. (1999, 2001) and Gray et al. (2003) describe granular flows, deflected by a solid obstacle to protect the area of the Schneefernerhaus at the Zugspitze (Eastern Alps, Germany). Hákonardóttir and Hogg (2005), Faug et al. (2007), Pudasaini et al. (2007) and Pudasaini and Kroener (2008) investigated the interaction between granular flows and deflecting obstacles. They observed an increasing flow depth (run up), where the granular flow hits the obstacle. The experiments on breaking mounds were performed by Hákonardóttir et al. (2001, 2003). It was observed that the mounds dissipate a large proportion of the kinetic energy of the granular flow. In Hauksson et al. (2007) and Cui and Gray (2013), experiments on differently shaped mast-like obstacles were carried out, focusing on the flow behavior in the area around a single mast. Granular flows hitting vertical impermeable obstacles are investigated in Faug et al. (2003, 2004a,b) and Caccamo et al. (2010), where it was shown that the local energy dissipation significantly accounts for the reduction of the runout length. Experiments on net structures were performed by Koegl et al. (2009), Koegl (2009) and Rammer et al. (2009), where the determined energy dissipation is remarkable. However, in these experiments no analysis of runout lengths was carried out, and therefore a further parameter study, which is presented in this paper, was deemed essential. In the current experiments graphite coated plastic granules are used in a 5 m long chute to generate granular flows, representing the dense part of an avalanche. Experiments with varying net mesh sizes, release volumes and chute inclinations are conducted and front velocities and flow depths are measured. In Section 2 the prototype of the Snowcatcher is described and an example of measured forces in a single event is shown. The performed lab experiments are presented in Section 3, while the results are discussed in Section 4.

2. Snowcatcher prototype

The goal of this paper is to better understand the interaction between moving snow and net structures. Field tests are restricted, because the repeatability of events is limited, and the effort of changing the Snowcatcher set-up is high. Notwithstanding these limitations, the data serves as a valuable source for analyzing the dynamic loading of steel net structures in a natural environment. It has been previously observed that rockfall nets were not only able to stop small avalanches, but also that parts of the net structure were damaged in case the snow loads exceeded the rockfall design loads (Margreth and Roth, 2006, 2008). Hence wire rope nets exposed to snow pressure and avalanches need an additional design procedure, accounting for these loads.

Measurements of dynamic forces in net structures due to avalanches are rare, therefore field tests were carried out. A full size prototype of the Snowcatcher was installed above a ski piste in Lech, Austria (Fig. 1). The avalanche path is SE exposed at an altitude of about 2200–2400 m a.s.l. The slope of the release zone is 35–45° and 20° at the position of the Snowcatcher. In contrast to rockfall nets that are constructed with swivel supports, the Snowcatchers supporting structures are made up of frames (Gleirscher et al., 2012; Rammer et al., 2009). Between 2008 and 2012 the installed system recorded data from 34 avalanche events.Based on the information of local experts the position for the Snowcatcher was chosen. The advantage of this site is the possibility of artificial avalanche release by explosives. Computational avalanche simulations with the software SamosAT (Sampl and Zwinger, 2004) showed pressure values in the range of 50 kN/m^2, which is defined as the design load for the Snowcatcher. Anyhow the structure is overdesigned in order to withstand higher pressures in case of larger avalanches. The prototype of the Snowcatcher consists of the following parts (Fig. 2):

- Omega-Net: This is the structure that catches the avalanche. It is a specially braided net, built to resist energies of up to 5000 kJ. The mesh width is in the range of 130–180 mm (red arrows).
- Cables: Bearing and middle ropes stretch the net and redirect forces from the structure to the lateral anchors (blue arrows).
- Brake elements: They expand at a certain force level and limit the load in the cables during an avalanche event (green arrows).

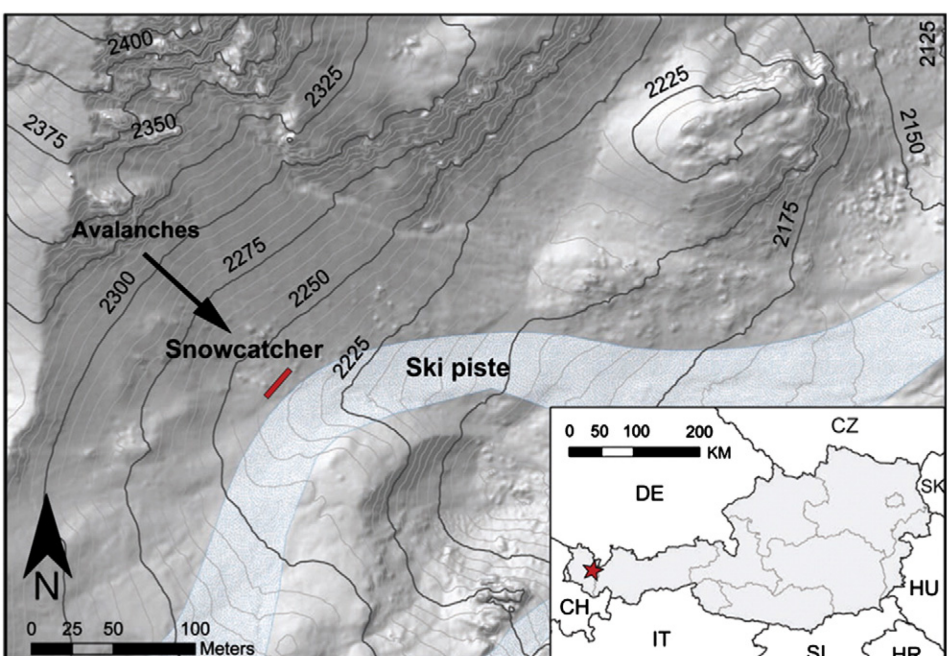

Fig. 1. Location of the test site in Lech.

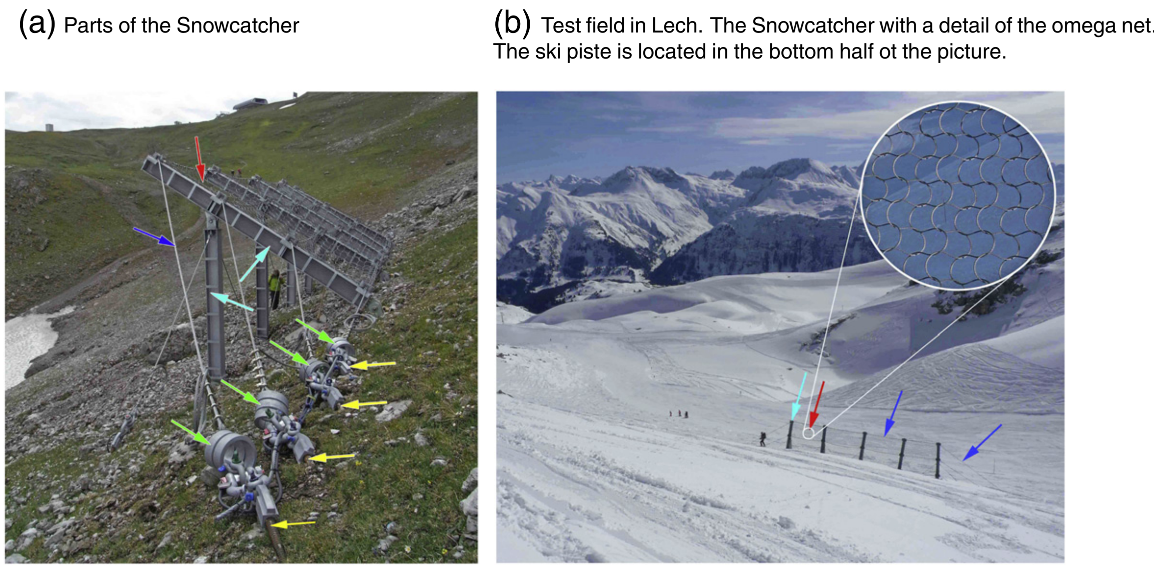

Fig. 2. Pictures of the Snowcatcher test field in summer (a) and winter (b). Red arrows mark the omega net, blue arrows the cables, green arrows the brake elements, cyan arrows the supporting frame and yellow arrows the anchors.

- Supporting structure: It is constructed as a three-hinged frame in the form of a λ (cyan arrows), called "Lambda frame".
- Anchors: IBO R51 anchors were used to transmit loads from cables and frames into the ground (yellow arrows).

Five Lambda frames were constructed at 4 m intervals, resulting in an overall width of the Snowcatcher prototype of 16 m. The height of the net supporting beam is 5.3 m and the angle of the beam to the terrain is 80°, whereas the terrain angle is in the range of 20°, see Fig. 3. Lower angles between net surface and terrain reduce the effective height of the system and complicate snow removal of avalanche deposit in the Snowcatcher by snow cats following an avalanche event. In contrast to currently implemented net structures, one advantage of the Snowcatcher is that there are no guy wires on the mountain side.

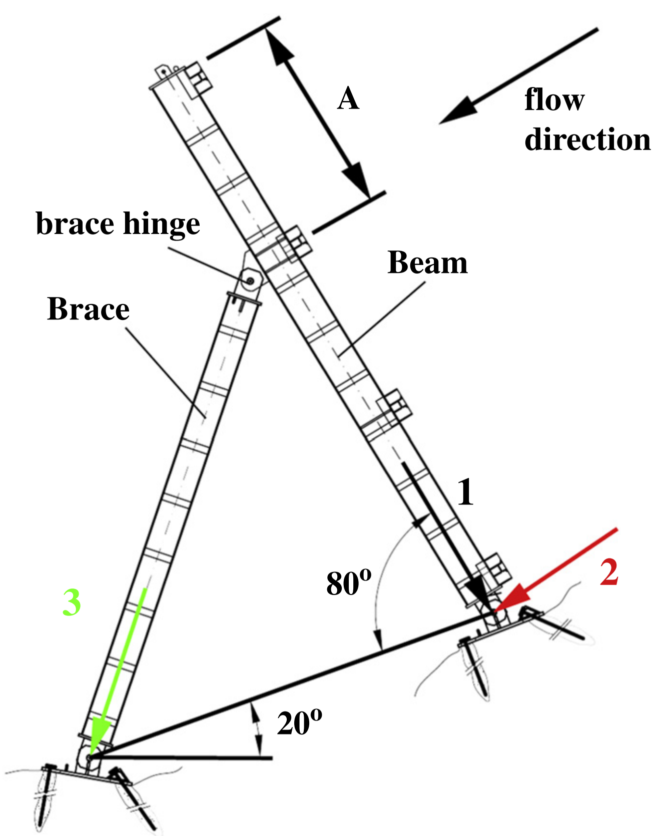

Fig. 3. Force measurement in the system. 1: normal force in the beam, 2: lateral force in the beam, 3: normal force in the brace.

2.1. Instrumentation

Several load measurement devices are installed in the system to record static forces caused by the snow cover as well as dynamic forces exerted by an avalanche. Two frames of the structure (1 frame in the middle and 1 frame at the edge) are instrumented with load measurement pins (Rainer et al., 2008). The colored arrows (Fig. 3) indicate the direction of the force measurement in the Snowcatcher. Data from all sensors is collected by data loggers with a rate of 20 Hz. Since there is no rapid change in the forces due to static loads of the snow cover, even in case of snowfall or snow melting, it is not necessary to continuously record all the data. The measurement of static forces takes place in an interval of 2 h. In case of an avalanche event, the forces in the structure rise rapidly. To measure this fast change the data is collected and saved with a rate of 20 Hz for a 3 minute period.

2.2. Measured avalanche events

In 4 years 24 avalanches were detected by the measurement system. None of the avalanches which impacted the Snowcatcher, did reach the ski piste. The largest forces were measured during an event on 21 January 2012. Fig. 4 shows the temporal development of the measured forces in the instrumented frames during this event. The given colors correspond to those in Fig. 3. The preceding snowfall and bad visibility prevented the collection of visual information of this event. Because of the strong precipitation during the winter of 2011/2012, the Snowcatcher was prefilled to two-thirds of its height. During this event two load peaks within 10 s were recorded in the force measurement. We assume the release of the first avalanche led to the initiation of a secondary avalanche that also hit the Snowcatcher. The two peaks in the middle frame equaled a normal force increase of 35 kN in the brace and 70 kN, respectively. At the edge frame however the first peak in the brace (45 kN) is larger than the second one (35 kN). Comparing

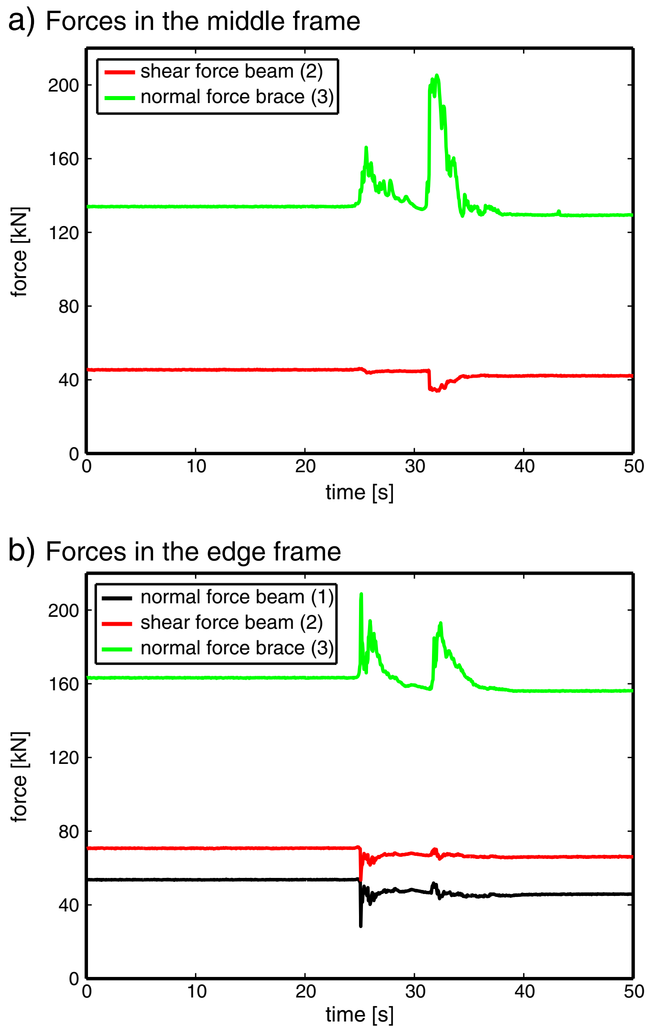

Fig. 4. Forces during an avalanche event in 2 frames. black: normal force in the beam(1), red: lateral force in the beam (2), green: normal force in the brace (3).

the magnitude of forces in the frames, the measurements indicate that the bulk of the first hit was closer to the edge frame and the bulk of the second hit closer to the middle frame. The normal force of the beam in the middle frame is missing, because of an electric overload during summer 2011.

Lateral forces in both frames are decreasing during the avalanche event. This force decrease at the bottom of the beam (Fig. 3, force 2) corresponds to a force within area A (Fig. 3) in flow direction, and arises due to a rotation around the brace hinge. In the edge frame the normal force in the beam shows an unloading of the beam. This unload may occur due to a drag exerted by a redirection of the avalanche flow towards the top of the beam. Static forces before the event due to the snow load were equal to 135 kN in the middle frame and 163 kN in the edge frame. The larger forces in the edge frame may be due to end-effect loads (Margreth et al., 2007). The static forces before the event are slightly bigger than those after the event. This might be due to an erosion of snow during the event. The design load of the Snowcatcher is 50 kN/m^2. Following basic static calculations (e.g. Schneider et al., 2006) a maximal allowed normal force of approximately 780 kN (design force) in the brace can be deduced. The avalanche event shown in Fig. 4 indicates a maximum force in the brace in the range of 210 kN, which is 27% of the design force. The maximum forces exerted on the brace, as recorded so far, were only one third of the design force.

3. Laboratory experiments

Granular experiments were carried out to examine the effectivity of the net barrier. The experiments were split into two parts: The investigation of the influence of i) the barrier angle and ii) the mesh size of the net.

3.1. Experimental set-up

The experiments were performed in a chute consisting of two 2.5 m long segments, the transit zone and the runout zone (Fig. 5). In the experiments, the inclination of the chute in the lower segment, α, is varied between 10°and 15°, while the inclination difference between the two segments remains constant at 20°. Similar experiments for granular channel flows were carried out and analyzed in detail by Wieland et al. (1999), Faug et al. (2003, 2004a,b), Pudasaini et al. (2007), Pudasaini and Kroener (2008), Faug et al. (2008), Pudasaini and Domnik (2009) and Cui and Gray (2013). However, these papers did not account for a granular flow being retarded by a net structure. The focus of this paper is to analyze the granular flow through a net, with a minimum of side wall effects due to friction. Therefore the granular flow was channelized in the transit zone. The shape of the transit zone is concave in the transversal direction (radius r = 2.1 m), whereas the runout zone is planar. The bed surface of the chute consists of smooth aluminum. On the surface of the chute a 5 cm × 5 cm grid is plotted for tracking the location of the flow front. The granular material is stored in a pipe with a diameter of 20 cm and a maximum volume of 30 liter. By pulling a cotter-pin, a flap opens abruptly and the material is released. Polystyrene particles are used in all experiments as a substitution material for avalanche snow. These particles are coated with a graphite layer to minimize electrostatic forces (Koegl et al., 2009). The particle diameters are in the range of 1.3–6.5 mm, where the smaller particles have a more spheric form, and the larger ones are more ellipsoids. The intersection of the transit and the runout zone is the position s of the net barrier where $s = 0$. Negative values refer to positions in the transit zone, positive values to positions in the runout zone. An overflow of the structure was studiously avoided. Consequently the granular flows never reached the height of the installed barrier. Particles passing the net barrier either flowed through the net or bypassed it laterally.

Two different set-ups were used to determine the influence of the net on the granular flow:

Set-up 1: Variation of the barrier angle

- net barrier width: 25% of the chute width (Fig. 5 top right); lateral bypass of the granular flow allowed.
- release mass: 2.75 kg
- net barrier angle β: 50°–70° (As the angle between the transit zone and the runout zone is constantly 20° and the barrier is situated in the intersection, $\beta = 60°$ corresponds to an angle of 80° between terrain and beam at the test site)
- mesh size: 10 mm

Set-up 2: Variation of mesh size

- net barrier width: 100% of the chute width (Fig. 5 bottom right); lateral bypass of the granular flow prevented.
- release mass: 6.50 kg
- net barrier angle β: 70°
- mesh sizes: 12 mm, 7 mm, 4 mm

3.2. Measurement devices and measured parameters

A video camera was installed above the chute to record the granular flow from the pipe exit to the runout zone. The camera recorded pictures with a frame rate of 29.97 fps. The front velocity v of the flow is determined by observing the location of the granular front parallel to the flow surface on each frame, using the 5 cm grid on the flow

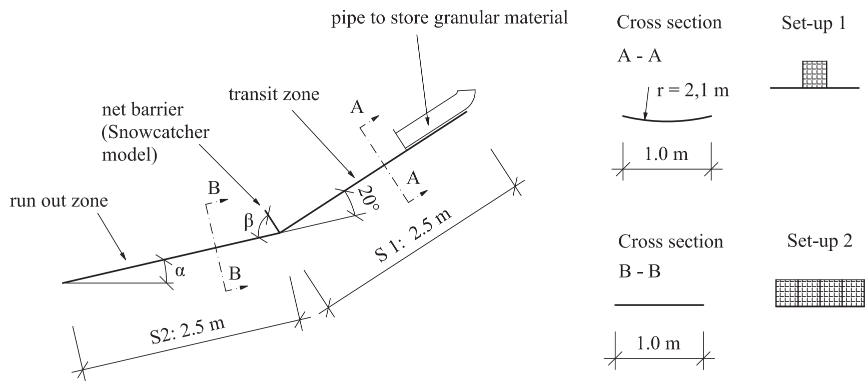

Fig. 5. Sketch of the experimental set-up. Left: side view of the chute, middle: cross sections of the segments, right: set-up of the net barriers.

surface as a spatial reference. Furthermore a distance sensor is installed to measure the flow depth h perpendicular to the flow surface. Similar measurements were also performed for granular flows down curved chutes by Pudasaini et al. (2005) in which the flow depth and the entire velocity profile was measured with PIV (Particle Image Velocimetry) measurement technique. The distance sensor operates with a frequency of 25 kHz. The measured parameters front velocity v and flow depth h allow the calculation of the Froude number

$$\mathrm{Fr} = \frac{v}{\sqrt{h\ g\ cos\theta}}, \tag{1}$$

where h corresponds to the maximum flow depth in time, g to the gravitational acceleration and θ to the slope inclination of the transit zone. The Froude number is an important dimensionless number that characterizes the dynamic of the flow and is defined as the ratio of inertial to potential energy. For a more detailed discussion on an extended Froude number, e.g. taking into account the apparent potential energy induced by gravity and pressure, we refer to Takahashi (2007), Pudasaini and Domnik (2009), and Domnik and Pudasaini (2012).

A Fast Fourier Transformation (FFT) was applied to the velocity and flow depth raw data to damper out fluctuations in the signals, after Brigham (1997). Because the video data and the laser data are recorded at different rates, the need degree of smoothing differs. The average of four similar experiments was compared to the smoothed curve of a single experiment. By keeping the difference between average curve and smoothed curve minimal, the degree of smoothing for further experiments was chosen. A cutoff frequency defines the intensity of smoothing. For the velocity data and the flow depth data a cutoff frequency of 5.0 Hz and 12.5 Hz is selected, respectively. Fig. 6 illustrates both raw and smoothed data for the velocity (a) and flow depth (b). By applying a FFT the detailed description at the beginning of the flow is lost. However, our analysis is based on the avalanche flow excluding starting and stopping phase. Therefore the smoothing by FFT seems to be adequate.

3.3. Dimensional analysis

In order to compare the granular experiments with avalanches in nature, the following criteria concerning geometry and dynamics have to be fulfilled.

- geometrical similarity

The mesh size of the full scale Snowcatcher is in the range of 130–180 mm. Assuming that the particle size in dry and wet natural avalanches is in the range of 65–162 mm (Bartelt and McArdell, 2009), the ratio d_{mesh}/d_{gran} in nature is in the range of 0.8–2.7. Mesh sizes of the obstacle in the experiments are between 4 and 12 mm. Since the granular material used in the experiments is 1.3–6.5 mm, the ratio d_{mesh}/d_{gran} is in the range of 0.6–9.2,which covers and even extends the natural range. Consequently even smaller particles, than observed in nature, are interacting with the net barrier.

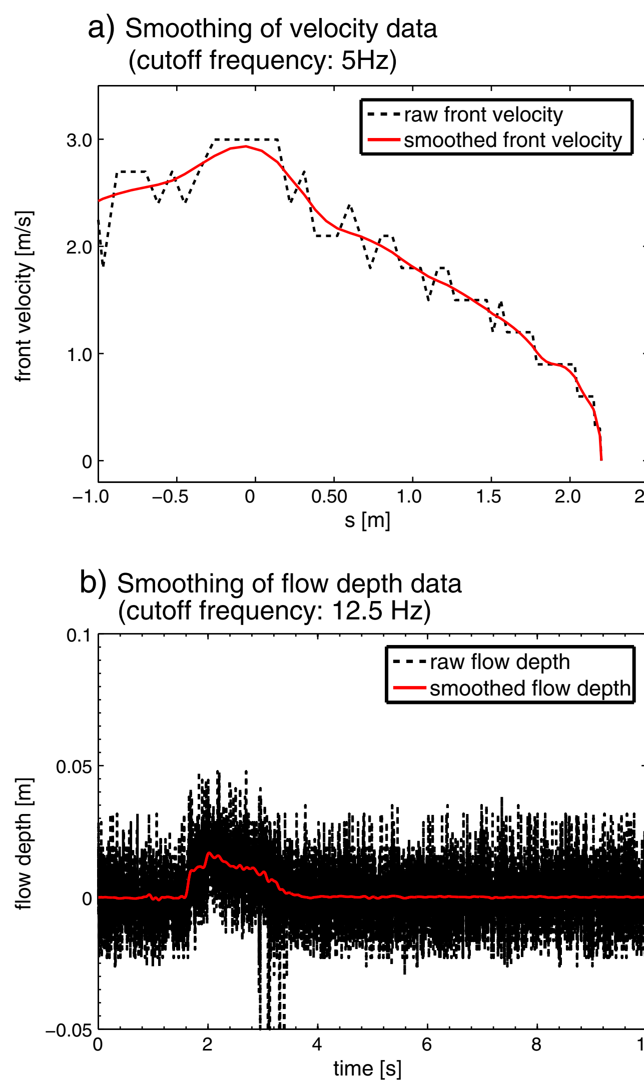

Fig. 6. FFT-smoothing of the experimental data. The data refers to an experiment with a release mass of 2.75 kg and a chute inclination angle α of 12°. No obstacle is installed to the chute.

The height of the Snowcatcher prototype is 5.3 m whereas the scaled obstacles are 0.35 m (h_{obs}) high. This refers to a scale of ca. 15:1.

- dynamical similarity

Densities in natural avalanches are between 80 kg/m^3 and 400 kg/m^3 (Dent et al., 1998). The bulk density of the material in experiments is 200 kg/m^3 (ρ). The Froude number is used as a measure of similitude between natural avalanches and granular flows. We determined Froude numbers within the experiments with 2.75 kg release mass at position $s = -0.10$ m. Here a distance sensor was installed in order to record the flow depth. Table 1 shows the calculated Froude numbers of the reference avalanches at this position. For natural avalanches at the Snowcatcher testsite, observations and estimations by local experts are in the range of $10 \le v \le 20$ m/s for velocities and $0.5 \le h \le 1.2$ m for flow depths. These ranges are in accordance with the results of the computational snow avalanche simulation software SamosAT. The slope angle in the Snowcatcher area is about 20°. This leads to calculated Froude numbers in the range of 3.1–9.5. Johannesson et al. (2009) refer to Froude numbers of the dense core of natural dry-snow avalanches between 5 and 10. Comparing the Froude numbers in Table 1 (7.1–8.6) to the expected in nature, the experimental values are at the upper limit. The aspect ratio $ar = h_{obs} / h_{max}$ (ratio between obstacle height and flow height) is shown in Table 1. The range of this value is 20–24 in the experiments and 4–10 for natural avalanches. The higher values of ar in the experiments result from smaller flow depths, that are likely to be higher for growing release volumes.

3.4. Reference avalanche experiments

To determine the effect of the net barrier, it is necessary to compare the experimental data with and without the installed net barrier. Experiments without the net barrier are defined as reference avalanches and are denoted with the subscript "ra". Fig. 7 illustrates the front velocities of the reference avalanches with different chute inclinations for a release mass of 2.75 kg. The abscissa refers to the location of the avalanche front, while the ordinate indicates the front velocity. Reference avalanches with α angles lower than 12° stop in the runout zone. For experiments with higher chute inclination the velocity increases and a part of the flow exceeds the length of the runout segment, compare Fig. 8. Reference avalanches with a release mass of 6.5 kg exceed the runout zone for all chute inclination angles, compare Fig. 9. The longer runout lengths are a result of the higher mass and the underlying size effect, which implies that larger masses generally travel farther than smaller ones (Erismann and Abele, 2001; Heim, 1932; Pudasaini and Hutter, 2007; Pudasaini and Miller, 2013).

3.5. Retardation length

The effectivity of the net barrier is determined by its retarding influence on the granular flow. To introduce a measure of effectivity, the retardation length (RL) is defined as the position $s = RL$, where the velocity v is equal to a threshold velocity v_{th}.

The threshold velocity value v_{th} is >0 m/s and has to be chosen according to the following limitations: (i) the stringent necessity of a

Table 1
Maximum velocities, maximum flow depths and corresponding Froude numbers in the transit zone at s = -0.10 m for the reference avalanches with release mass of 2.75 kg.

α [°]	v_{max} [m/s]	h_{max} [m]	$Fr_{10_{ra}}$ [–]	ar [–]
10	2.48	0.015	7.1	23.3
11	2.62	0.015	7.7	23.3
12	2.94	0.017	8.1	20.6
13	2.77	0.015	8.1	23.3
14	3.02	0.017	8.5	20.6
15	2.96	0.016	8.6	21.9

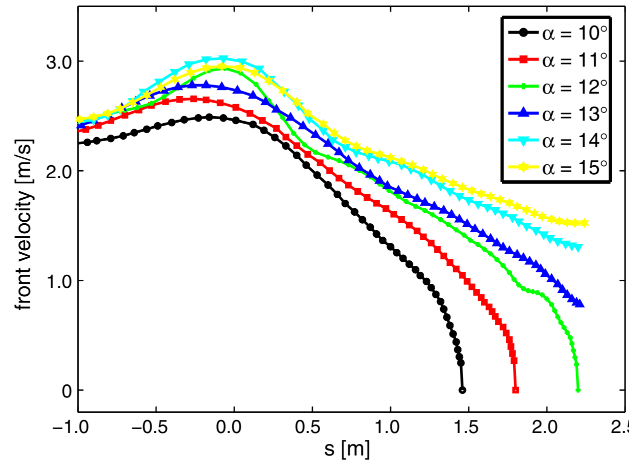

Fig. 7. Front velocities of granular reference avalanches with a release mass of 2.75 kg.

front location in the runout zone, meaning that the intersection of the front velocity curve with the threshold velocity must be in the range of $0 \le s \le 2.5$ m, compare Figs. 8 and 9; (ii) minimizing the effects of diffluence on the retardation length. In natural avalanches cohesion is most apparent near standstill and prevents diffluence of the avalanching material (Pudasaini and Hutter, 2007). In the laboratory experiments diffluence appears near standstill, due to lacking cohesion. It is expressed by an abrupt acceleration of the granular material for small front velocities, compare Figs. 8 and 9.

The value of v_{th}, displayed as a dashed line in Figs. 8 and 9, influences the absolute values of retardation lengths. In this paper, the focus is on the effectivity of the barrier, which is defined as the ratio of retardation lengths with and without barrier. Thus, absolute values of retardation lengths may differ for different threshold velocities, but the value of the effectivity is rather unaffected. For our experimental set-up it was appropriate to choose the threshold velocity v_{th} as a constant value:

$$v_{th} = 1.85 \text{ m/s}.$$

Fig. 10 shows the retardation lengths of reference avalanches for different chute inclinations and release masses. Black crosses denote experiments with 2.75 kg, and red circles denote experiments with 6.5 kg release mass. Obviously retardation lengths increase with increasing chute angles. Experiments with 2.75 kg release mass result in smaller retardation lengths than experiments with 6.50 kg, which is in accordance with the presence of a size effect advocated by (Erismann and Abele, 2001; Heim, 1932; Pudasaini and Hutter, 2007; Pudasaini and Miller, 2013). The difference of retardation lengths between experiments with 2.75 kg and 6.50 kg raises with increasing chute angle and is in the range of 20–30%.

3.6. Comparison of retardation lengths in set-up 1

Fig. 8 shows the front velocities of the reference avalanche (triangles) and front velocities of flows through the net barrier for different chute inclinations. Differences of front velocities in the transit zone ($s < 0$), that are observed over all experiments (compare Figs. 8 or 9), are attributed to properties of the granular flow itself and measurement inaccuracies. The measurement of front velocities includes variations that arise due to turbulences that occur in the avalanche head (Koegl et al., 2009). Furthermore different initial conditions such as varying intermixture (spatial particle size distribution in the release pipe) of release mass and precision of setting the chute angle α or air humidity could influence the results. In Fig. 8 the reference avalanches are

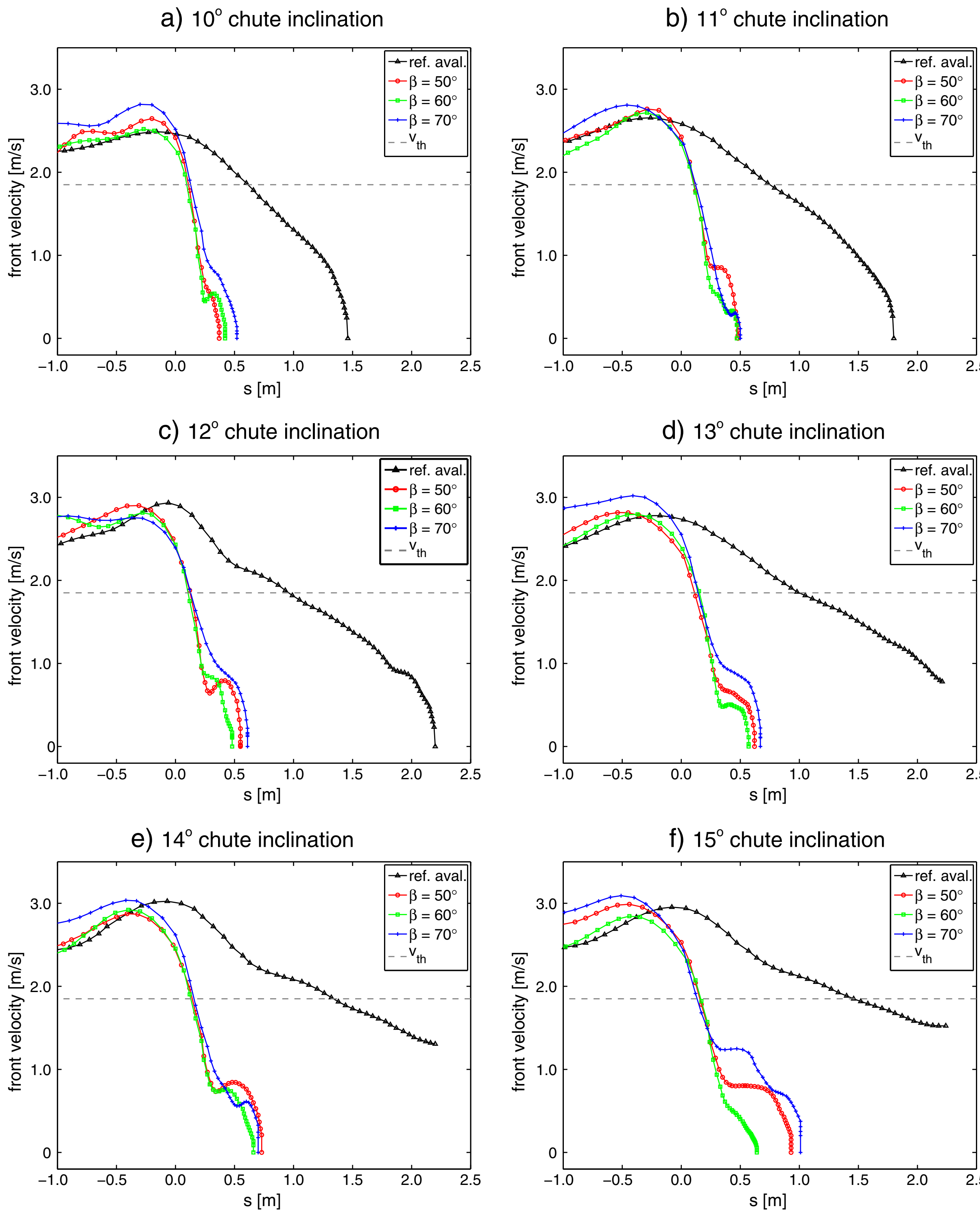

Fig. 8. Effect of different β angles in experiments with different chute inclination α. The lines refer to the reference avalanche and the flow interacting with the net. Dashed lines correspond to the threshold velocity v_{th}. Release mass: 2.75 kg.

compared to the granular flows directly interacting with the net. Table 2 illustrates retardation lengths for the threshold velocity of $v_{th} = 1.85$ m/s for flows shown in Fig. 8. The indices "ra", "β50", "β60" and "β70" denote the reference avalanche and the corresponding net barrier angles, respectively. The comparison of the retardation lengths indicates slightly smaller values for barrier angles β of 50° and 60°, than for 70°.

3.6.1. Influence of barrier angle β for different chute inclinations

The results displayed in Table 2 are visualized in Fig. 11. For a better interpretation a first order regression is performed. The slopes of the regression lines show an obvious negative slope for increasing chute angles. In other words, with higher chute inclinations, which generally correspond to higher Froude numbers (Table 1), the effectivity of the net barrier increases. For higher chute inclinations, the differences due

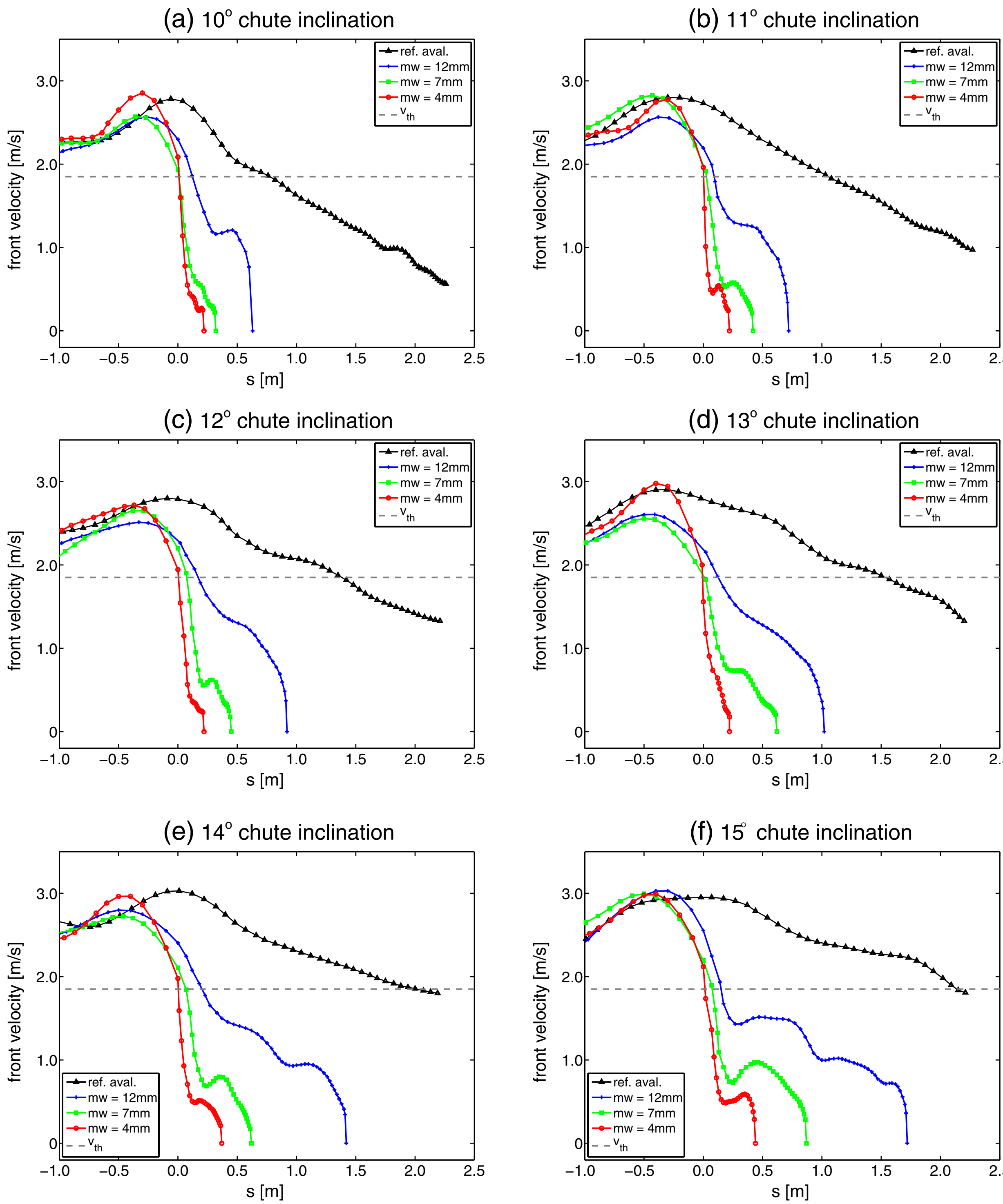

Fig. 9. Effect of different mesh widths in experiments with different chute inclination α. Release mass: 6.50 kg.

to the barrier angle β decreases. This indicates that the net barrier angle between 50° and 70° has a decreasing influence on the retardation with increasing chute angles. This means that the net barrier angle in the presented experiments had a minor influence on flows with higher Froude numbers. Generally, different results are observed for experiments with different barrier angles β. For smaller chute angles, high β angles appear to correspond to lower effectivity.

3.6.2. Effects of particle size and effective mesh size

One possible explanation for the observation of longer retardation lengths with $\beta = 70°$ at lower chute inclination angles is the magnitude of d_{eff}, the "effective mesh width". Imagining a plane perpendicular to the undisturbed flow direction, the projected mesh width on this plane is smaller for all angles deviating from 90°. Fig. 5 shows that a barrier angle of 70° refers to a 90° barrier to the flow direction. Hence the effective mesh width is maximal and leads to longer

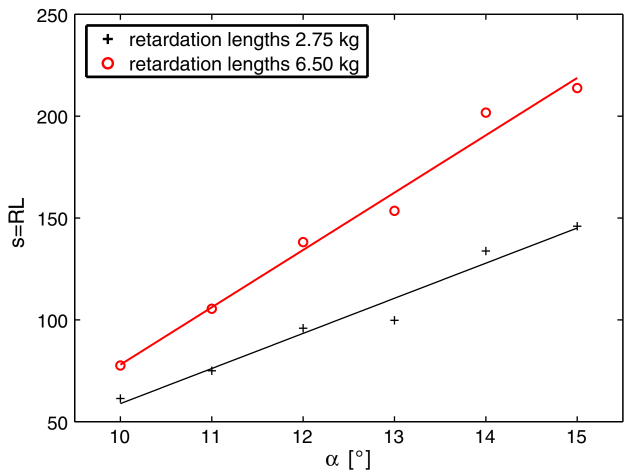

Fig. 10. Retardation lengths of reference avalanche experiments with 2.75 kg and 6.50 kg release mass.

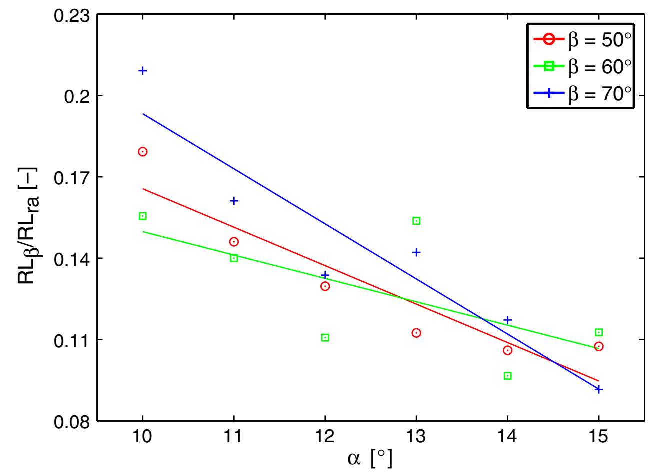

Fig. 11. Ratio of retardation lengths of flows through the net surface (RL_β) and the retardation lengths of the reference avalanche (RL_{ra}) at different chute inclinations.

retardation lengths compared to other barrier angles. A significant difference between experiments with barrier angles of 50° and 60° due to the effective mesh width cannot be observed.

To quantify this effect, the ratio of the effective mesh width d_{eff} and the maximal diameter of the granular material $dg = 6.5$ mm is compared to the ratio of the retardation lengths in Table 2. The maximum diameter of the granular material is chosen as a reference, because larger particles tend to be at the front of granular flows (Félix and Thomas, 2004; Hutter and Rajagopal, 1994; Kern, 2000), and are therefore crucial for the first interaction with the net. A superimposed box plot in Fig. 12 provides basic statistical information such as median and 25%/75% quartiles as well as outliers. Experiments with a barrier angle of 70° show larger variations in the results than experiments with 50° or 60° respectively. Retardation lengths of flows interacting with the net are reduced by 12%, 13% and 14% (median values) of the corresponding reference avalanche, for experiments with $\beta = 50°$, $\beta = 60°$ and $\beta = 70°$, respectively. The maximum and minimum ratio of the retardation length to the reference retardation length are 9% and 21% respectively. However, these results have to be interpreted with care, since the number of experiments is limited and the effect diminishes or even reverses for high chute inclinations. Furthermore the magnitude of front velocity differences in the undisturbed transit zone is in a similar range as the observed effect. Thus these variations maybe attributed to variations in the granular flow itself as well as measurement inaccuracies (e.g. intermixture, material properties).

With the choice of an optimum β one has to consider, that a lower angle leads to higher effectivity for flows with small Froude numbers, but the effective height of the barrier (perpendicular to the flow surface) decreases.

3.7. Comparison of retardation lengths with set-up 2

To further study the effect of mesh size on the effectivity, additional experiments are performed. Fig. 9 illustrates the comparison of velocities

Table 2
Retardation lengths [m] of granular flows with 2.75 kg release mass.

α	RL_{ra}	$RL_{\beta 50}$	$RL_{\beta 60}$	$RL_{\beta 70}$
10°	0.61	0.11	0.10	0.13
11°	0.75	0.11	0.11	0.12
12°	0.96	0.12	0.11	0.13
13°	1.00	0.11	0.15	0.14
14°	1.34	0.14	0.13	0.16
15°	1.46	0.16	0.16	0.13

in experiments with different chute inclination angles and mesh size. Table 3 lists the corresponding retardation lengths. The indices “ra”, “mw12”, “mw7” and “mw4” denote the reference avalanche and the experiments corresponding to the different mesh widths, respectively. Comparing the results in Table 3, a reduction of the retardation lengths caused by the net is obvious in all experiments.

3.7.1. Influence of mesh size

Fig. 13 shows the dependence of the retardation length ratio RL_{mw}/RL_{ra} on the chute inclination angle α. The smaller the mesh size, the more the net barrier acts like a dam, leading to retardation lengths of zero, which corresponds to maximum effectivity. Experiments with mesh sizes of 12 mm show an increasing effectivity with increasing chute inclination, which corresponds to increasing Froude numbers of the flow. In comparison, experiments with mesh sizes 4 mm and 7 mm indicate a less or even opposing dependence on the chute inclination, respectively on the Froude number. This suggests that for the mesh sizes 4 mm and 7 mm the net barrier tends to clog and therefore acts as an impermeable surface.

3.7.2. Influence of the particle diameter and mesh size

In Fig. 14, the ratio of the mesh width d_{mesh} to the maximal diameter of the granular material d_g is compared to the ratio of retardation

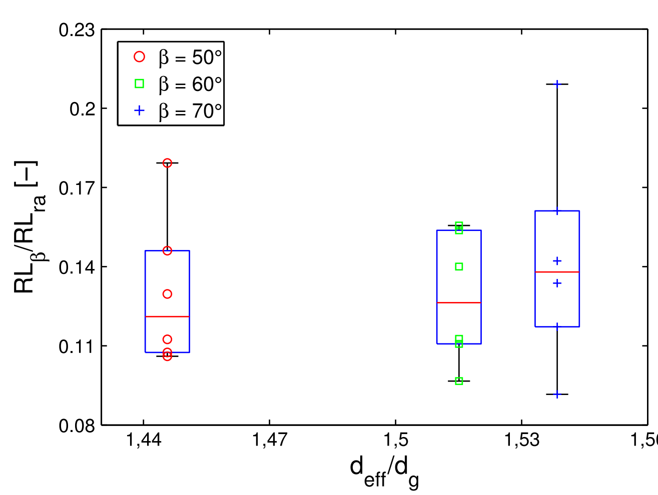

Fig. 12. Influence of the maximal particle diameter and the effective mesh size on the normalized retardation length. The central mark of the box plot is the median, the edges of the box are the 25th and 75th percentiles, the whiskers extend to the outliers.

Table 3
Retardation lengths [m] of granular flows with 6.50 kg release mass.

α	RL_{ra}	RL_{mw12}	RL_{mw7}	RL_{mw4}
10°	0.78	0.12	0.01	0.01
11°	1.05	0.09	0.03	0.00
12°	1.38	0.17	0.07	0.00
13°	1.54	0.13	0.01	0.00
14°	2.02	0.20	0.07	0.00
15°	2.14	0.15	0.07	0.01

lengths. A superimposed box plot provides basic statistical information such as median and 25%/75% quartiles as well as outliers.

Observing a decreasing effectivity with increasing mesh size, the results of set-up 2 confirm the results of set-up 1. Retardation lengths of flows interacting with the net are reduced to 1%, 3% and 10% of the corresponding reference avalanche, revealing a higher effectivity with decreasing mesh size. The variation of the results is increasing for larger mesh sizes. In experiments with 6.50 kg release mass, the retardation length is at least reduced to 16% compared to the reference avalanches.

4. Discussion and conclusion

This paper is an attempt to better understand the interaction of snow avalanches with net structures. We want to provide a first step in analyzing the retarding effect of steel wire rope nets on granular flows. Motivated by field tests that showed the magnitude of forces in parts of the Snowcatcher due to small avalanches, different experiments were performed in the lab.

The influence of the β angle and the mesh size on the retardation of a granular flow was analyzed in lab experiments. In 48 experiments front velocities were measured. As a measure of effectivity, the retardation lengths of the flow for a defined threshold velocity are determined and compared. This threshold velocity accounts for a lacking cohesion in the experiments. The results indicate that effectivity increases with higher chute inclination, which correspond to higher Froude numbers. Experiments with different barrier angles β showed that higher chute inclination angles lead to higher effectivities of the barrier. Additionally the effective mesh size influences the retardation length. Increasing effective mesh sizes leads to larger retardation lengths, which corresponds to a lower effectivity of the net barrier.

Experiments with different mesh sizes indicate a velocity dependency of the effectivity at a certain ratio of mesh to grain size. Mesh sizes in the range of 1.5–2 times the maximal grain size, indicate a velocity dependence of the net structures effectivity. More precisely, the effectivity of the net barrier increases with higher chute angles, corresponding to higher Froude numbers. Comparing experiments with and without net

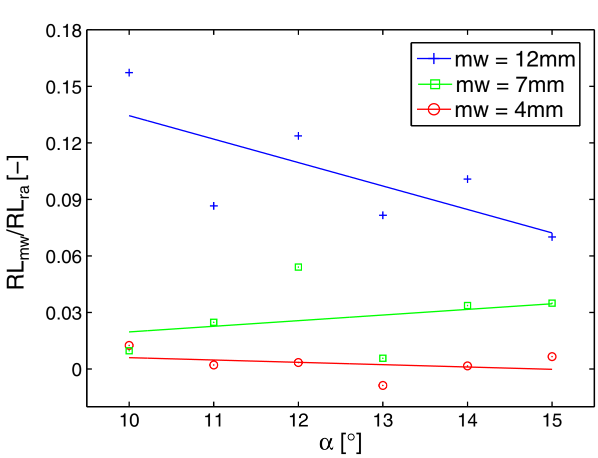

Fig. 13. Ratio of retardation lengths of flows through different mesh sizes (RL_{mw}) and the retardation length of the reference avalanche (RL_{ra}) at various chute inclinations.

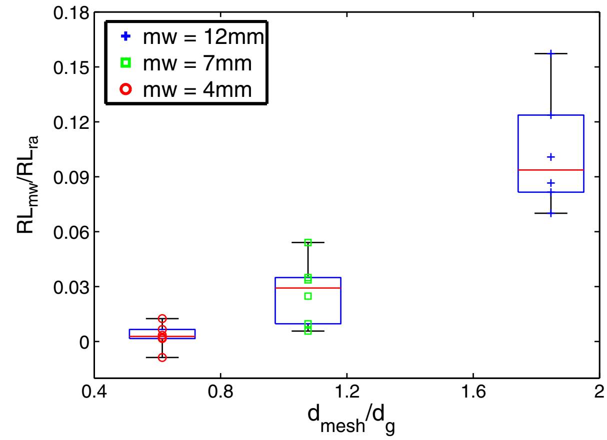

Fig. 14. Influence of the maximal particle diameter and the mesh size on the normalized retardation length. The central mark of the box plot is the median, the edges of the box are the 25th and 75th percentiles, the whiskers extend to the most extreme data points.

barrier, a retardation length reduction of at least 79% was observed. For mesh sizes in the range of the maximum grain size, the experiments in set-up 2 show an independence of the normalized retardation lengths from higher chute angles (Fig. 13). Due to small mesh sizes, the net tends to behave less permeable and therefore acts like a dam. The influence of the net surface inclination on the normalized retardation length is in the range of 2% in the experiments, which seems to be negligible.

Further research is required in order to investigate the comparability of scaled lab experiments and field measurements. Under natural circumstances, e.g. prefilling of the barrier leads to an overflow or lateral bypass, which is not considered in the experiments. Due to unknown parameters (e.g. lubrication, fluidisation, etc., see Pudasaini and Hutter, 2007; Pudasaini and Miller, 2013), as well as a small sample size, the presented results have to be interpreted with care, but are promising as a first step. The presented methods and results can also be applied to other types of mass flows and avalanches, such as rockfall or debris flows (see e.g. Bichler et al., 2012; Pudasaini, 2012; Wendeler et al., 2006).

Acknowledgments

This project was carried out with support of the FFG (Österreichische Forschungsförderungsgesellschaft; Project number: 815444), the Trumer Schutzbauten Gmbh, the Bergbahnen Lech and the Unit of Hydraulic Engineering (University Innsbruck). The assistance from Thomas Gigele, Armin Graf, Klaus Suntinger and the whole Unit of Snow and Avalanches (BFW) is gratefully acknowledged. We thank the two reviewers and the editor for their valuable comments which helped to increase clarity and quality of this paper.

References

Baillifard, M.-A., 2007. Interaction Between Snow Avalanches and Catching Dams. (PhD thesis) ETH Zurich.
Bartelt, P., McArdell, B., 2009. Granulometric investigations of snow avalanches. J. Glaciol. 55 (193), 829–833.
Bichler, A., Yonin, D., Stelzer, G., 2012. Flexible debris flow mitigation: introducing the 5.5 mile debris fence. Landslides and Engineered Slopes: Protecting Society Through Improved Understanding, pp. 1209–1214.
Brigham, E.O., 1997. FFT-Anwendungen. Oldenbourg.
Caccamo, P., Chanut, B., Faug, T., Bellot, H., Naaim-Bouvet, F., 2010. Small-scale laboratory tests on granular avalanches overflowing a flat obstacle: flow regimes, dead zone and induced forces. Proceedings of the EPFL Doctoral Conference in Mechanics.
Cui, X., Gray, J., 2013. Gravity-driven granular free-surface flow around a circular cylinder. J. Fluid Mech. 720, 314–337.
Dent, J., Burrell, K., Schmidt, D., Louge, M., Adams, E., Jazbutis, T., 1998. Density, velocity and friction measurements in a dry-snow avalanche. Ann. Glaciol. 26, 247–252.
Domaas, U., Harbitz, C., Bakkehøi, H., 2002. The EU CADZIE database for extreme and deflected snow avalanches. Nat. Hazard. Earth Syst. Sci. 2, 227–238.

Domnik, B., Pudasaini, S.P., 2012. Full two-dimensional rapid chute flows of simple viscoplastic granular materials with a pressure-dependent dynamic slip-velocity and their numerical simulations. J. Non-Newtonian Fluid Mech. 173, 72–86.

Erismann, T., Abele, G., 2001. Dynamics of Rockslides and Rockfalls. Springer, Berlin Heidelberg New York.

Faug, T., Naaim, M., Bertrand, D., Lachamp, P., Naaim-Bouvet, F., 2003. Varying dam height to shorten the run-out of dense avalanche flows: developing a scaling law from laboratory experiments. Surv. Geophys. 24, 555–568.

Faug, T., Naaim, M., Naaim-Bouvet, F., 2004a. An equation for spreading length, center of mass and maximum run-out shortenings of dense avalanche flows by vertical obstacles. Cold Reg. Sci. Technol. 39, 141–151.

Faug, T., Naaim, M., Naaim-Bouvet, F., 2004b. Experimental and numerical study of granular flow and fence interaction. Ann. Glaciol. 38, 135–138.

Faug, T., Naaim, M., Fourriére, A., 2007. Dense snow flowing past a deflecting obstacle: an experimental investigation. Cold Reg. Sci. Technol. 49 (1), 64–73.

Faug, T., Gauer, P., Lied, K., Naaim, M., 2008. Overrun length of avalanches overtopping catching dams: cross-comparison of small-scale laboratory experiments and observations from full-scale avalanches. J. Geophys. Res. 113 (F3), F03009.

Félix, G., Thomas, N., 2004. Relation between dry granular flow regimes and morphology of the deposits: formation of levées in pyroclastic deposits. Earth Planet. Sci. Lett. 221, 197–213.

Gleirscher, E., Fischer, J.-T., Rainer, E., Stelzer, G., Rammer, L., Kern, M., 2012. SNOWCATCHER: a new snow avalanche protection measure. International Snow Science Workshop, Anchorage, Alaska.

Gottardi, G., Govoni, L., 2010. Full-scale modelling of falling rock protection barriers. Rock Mech. Rock. Eng. 43 (3), 261–274.

Gray, J.M.N.T., Tai, Y.C., Noelle, S., 2003. Shock waves, dead zones and particle-free regions in rapid granular free-surface flows. J. Fluid Mech. 491 (1), 161–181.

Hákonardóttir, K., 2004. The Interaction Between Snow Avalanches and Dams. (PhD thesis) University of Bristol, School of Mathematics, Bristol, England.

Hákonardóttir, K., Hogg, A., 2005. Oblique shocks in rapid granular flows. Phys. Fluids 17, 077101.

Hákonardóttir, K., Jóhannesson, T., Tiefenbacher, F., Kern, M., 2001. A Laboratory Study of the Retarding Effect of Breaking Mounds in 3, 6 and 9 m Long Chutes. Veurstofa Íslands.

Hákonardóttir, K., Hogg, A., Jóhannesson, T., Tómasson, G., 2003. A laboratory study of the retarding effects of braking mounds on snow avalanches. J. Glaciol. 49 (165), 191–200.

Hauksson, S., Pagliardi, M., Barbolini, M., Jóhannesson, T., 2007. Laboratory measurements of impact forces of supercritical granular flow against mast-like obstacles Cold Reg. Sci. Technol. 49 (1), 54–63.

Heim, A., 1932. Bergsturz und Menschenleben. Beiblatt zur Vierteljahresschrift der Naft. Ges. Zürich, 20 1–218.

Hutter, K., Rajagopal, K.R., 1994. On flows of granular materials. Contin. Mech. Thermodyn. 6, 81–139.

Johannesson, T., Gauer, P., Issler, D., Lied, K. (Eds.), 2009. The design of avalanche protection dams. Recent practical and theoretical developments. European Commision. Directorate General for Research (M. Barbolini and U. Domaas and C. B. Harbitz and T. Johannesson and P. Gauer and D. Issler and K. Lied and T. Faug and M. Naaim and F. Naaim-Bouvet and K. M. Hakonardottir and L. Rammer).

Kern, M., 2000. Inverse Grading in Granular Flow. (PhD thesis) École Polytechnique Fédérale de Lausanne.

Koegl, J., 2009. Simulation von turbulenten Fließlawinen im physikalischen Modell. (Master's thesis) Leopold-Franzens-Universität Innsbruck.

Koegl, J., Graf, A., Rammer, L., Kleemayr, K., Kern, M., Gauer, P., Kapeller, G., Aufleger, M., 2009. Scaled laboratory experiments on the evolution of fluidised avalanches. Proceedings ISSW Davos.

Margreth, S., Roth, A., 2006. Interaction of flexible rockfall barriers with avalanches and snow pressure. International Snow Science Workshop (ISSW), Telluride Colorado.

Margreth, S., Roth, A., 2008. Interaction of flexible rockfall barriers with avalanches and snow pressure. Cold Reg. Sci. Technol. 51, 168–177.

Margreth, S., et al., 2007. Lawinenverbau im Anbruchgebiet. Technische Richtlinie als Vollzugshilfe.Bundesamt für Umwelt, Bern.

Margreth, S., Suda, J., Hofmann, R., Gauer, P., Sauermoser, S., Schilcher, W., Skolaut, C., 2011. Permanenter Technischer Lawinenschutz: Bemessung und Konstruktion. In: Rudolf-Miklau, F., Sauermoser, S. (Eds.), Handbuch Technischer Lawinenschutz.

Nicot, F., Boutillier, B., Meyssonnier, J., Gagliardini, O., Darve, F., 2004. Modelling the mechanical interaction between flowing materials and retaining wire structures. Comput. Geotech. 31 (6), 427–441.

Peila, D., Ronco, C., 2009. Technical note: design of rockfall net fences and the new ETAG 027 European guideline. Nat. Hazard. Earth Syst. Sci. 9 (4), 1291–1298.

Pudasaini, S.P., 2012. A general two-phase debris flow model. J. Geophys. Res. 117 (F3), F03010.

Pudasaini, S.P., Domnik, B., 2009. Energy considerations in accelerating rapid shear granular flows. Nonlinear Process. Geophys. 16 (3), 399–407.

Pudasaini, S.P., Hutter, K., 2007. Avalanche Dynamics: Dynamics of Rapid Flows of Dense Granular Avalanches. Springer, Berlin, New York.

Pudasaini, S.P., Kroener, C., 2008. Shock waves in rapid flows of dense granular materials: theoretical predictions and experimental results. Phys. Rev. E 78 (4), 041308.

Pudasaini, S.P., Miller, S.A., 2013. The Hypermobility of Huge Landslides and Avalanches. Engineering Geology.

Pudasaini, S., Hsiau, S., Wang, Y., Hutter, K., 2005. Velocity measurements in dry granular avalanches using particle image velocimetry technique and comparison with theoretical predictions. Phys. Fluids 17, 093301.

Pudasaini, S., Hutter, K., Hsiau, S., Tai, S., Wang, Y., Katzenbach, R., 2007. Rapid flow of dry granular materials down inclined chutes impinging on rigid walls. Phys. Fluids 19, 053302.

Rainer, E., Rammer, L., Wiatr, T., 2008. Snow loads on defensive snow net systems. International Symposium on Mitigative Measures against Snow Avalanches, Egilsstair, Iceland.

Rammer, L., Stelzer, G., Kern, M., 2009. Investigation on the effectiveness of the catch-fence “Snowcatcher” as avalanche protection system. ISSW — International Snow Science Workshop.

Roth, A., Wendeler, C., Amend, F., 2010. Use of properly designed flexible barriers to mitigate debris flow natural hazards. Proceedings of GeoFlorida 2010: Advances in Analysis, Modeling and Design, West Palm Beach, Florida, USA, 20–24 February 2010. American Society of Civil Engineers (ASCE), pp. 3207–3216.

Sampl, P., Zwinger, T., 2004. Avalanche simulation with SAMOS. Ann. Glaciol. 38 (1), 393–398.

Schneider, K.-J., Goris, A., Albert, A., 2006. Bautabellen für Ingenieure: mit Berechnungshinweisen und Beispielen. Werner Verlag.

Tai, Y.-C., Wang, Y., Gray, J., Hutter, K., 1999. Methods of similitude in granular avalanche flows. Advances in Cold-Region Thermal Engineering and Sciences. 415–428.

Tai, Y.C., Gray, J.M.N.T., Hutter, K., Noelle, S., 2001. Flow of dense avalanches past obstructions. Ann. Glaciol. 32, 281–284.

Takahashi, T., 2007. Debris Flows: Mechanics, Predictions and Countermeasures. Taylor & Francis, New York.

Volkwein, A., 2005. Numerical simulation of flexible rockfall protection systems. Proc. Computing in Civil Engineering.

Wendeler, C., McArdell, B., Rickenmann, D., Volkwein, A., Roth, A., Denk, M., 2006. Field testing and numerical modeling of flexible debris flow barriers. Proc. Int. Conf. on Physical Modelling in Geotechnics, Honkong.

Wieland, M., Gray, J.M.N.T., Hutter, K., 1999. Channelized free-surface flow of cohesionless granular avalanches in a chute with shallow lateral curvature. J. Fluid Mech. 392, 73–100.